# Naked-Eye Detection of C1–C4 Alcohols Based on Ground-State Intramolecular Proton Transfer

**ARTICLE** *in* ANALYTICAL CHEMISTRY · FEBRUARY 2014

Impact Factor: 5.64 · DOI: 10.1021/ac403550t · Source: PubMed



**7 AUTHORS**, INCLUDING:

Zhan-Xian Li
Zhengzhou University
**47** PUBLICATIONS **718** CITATIONS
SEE PROFILE

Ming-Ming Yu
Zhengzhou University
**62** PUBLICATIONS **507** CITATIONS
SEE PROFILE

analytical chemistry

Article

pubs.acs.org/ac

# Naked-Eye Detection of C1−C4 Alcohols Based on Ground-State Intramolecular Proton Transfer

Zhanxian Li,* Xingjiang Liu, Wanying Zhao, Sheng Wang, Wan Zhou, Liuhe Wei, and Mingming Yu*

The College of Chemistry and Molecular Engineering, Zhengzhou University, Zhengzhou 450001, China

Supporting Information

**ABSTRACT:** Previous reports of fluorescent sensors for alcohols based on charge-transfer character of their excited state are based on mono-, di-, and tetra-phosphonate cavitands, which are capable of selecting analytes through shape/size selection and various specific H-bonding, CH−$\pi$, and cation−dipole interactions. To contrast, color changes based on absorption properties of the ground state are more suitable for direct observation with the naked eye. Three sensitive and selective colorimetric sensors for C1−C4 alcohols have been developed on the basis of alcohol-mediated ground-state intramolecular proton transfer. Reverse proton transfer induced by water achieves a fully reversible reaction. In addition, the solvent color indicates alcohol concentration.

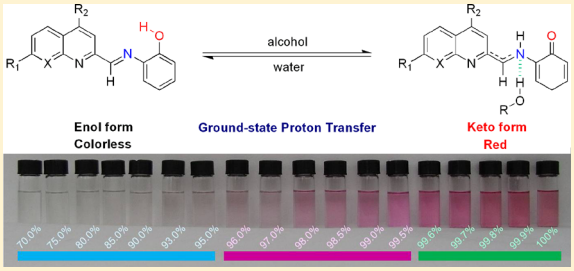


In recent years, considerable research efforts have been directed to developing sensors specific for different classes of analytes, and it is still necessary to obtain novel chemical sensors for detection of chemical species.[1] Among them, previous reports of fluorescent sensors for alcohols based on charge-transfer character of their excited state are based on mono-,[2] di-,[3] and tetraphosphonate cavitands,[4] which are capable of selecting analytes through shape/size selection and various specific H-bonding, CH−$\pi$, and cation−dipole interactions.[5] H-bonding with one of the P═O groups and CH−$\pi$ interactions with the $\pi$-basic cavity perturb the selectivity pattern between the analyte and the cavitand layer by adding their contribution to the sensor responses. The number of inward-facing P═O groups enhances the sensor response through entropic stabilization of the alcohol−cavitand complexes via energetically equivalent multiple interactions.[6]

As one of the most important chelators for metal ions, 8-hydroxyquinoline (8-HQ) and its derivatives have been used as fluorescent sensors for cellular and environmental metal ions, because metal binding to 8-HQ can block the excited-state intramolecular proton transfer (ESIPT) channel and restore the fluorescence.[7] 1,8-Naphthyridine and its derivatives have been widely used as guanine recognition regents,[8] for supramolecular assembly of multiple hydrogen-bonded units,[9] and as bidentate ligands for constructing short metal−metal distance building blocks[10] or transition metal complexes involving Ru(II), Mn(III), Ir(III), and other metals as water oxidation catalysts.[11] Our group has developed fluorescent chemosenors of metal ions based on their various photoluminescent and chelating properties.[12]

Proton transfer plays a critical role in many chemical, photochemical, catalytic, and biomolecular processes as the most basic and important biological and chemical process; it is also a hot topic in today's scientific research.[13] Proton transfer reactions can be classified and identified by the reaction in the ground or excited states, strong or weak hydrogen bonding, driving forces based on acidity and basicity, etc.[14] On the basis of the ESIPT mechanism, various fluorometric sensors have been developed because of their unique and outstanding spectral sensitivity to the environmental medium.[15] Ground-state tautomerism including ground-state reverse proton transfer (GSRPT) process after excited-state proton transfer was investigated by theoretical methods[16] and spectroscopic techniques.[17] The phenomenon of enol−keto tautomeric transformation in the ground state involving the transfer of hydroxyl proton to the imidazole has been observed.[18] Up to now, to the best of our knowledge, there has been no example of sensors based on ground-state intramolecular proton transfer reported.

Fluorescent sensors normally depend on emission intensity or position change and could be significantly influenced by excitation power and detector sensitivity. To contrast, color changes based on absorption properties of the ground state are more suitable for direct observation with the naked eye.[19] In this paper, we report C1−C4 short-chain alcohol naked-eye sensors based on ground-state intramolecular proton transfer and tautomerism strategies. To achieve this goal, new 1,8-naphthyridine, 8-hydroxyquinoline, and 2-aminophenol derivatives (Figure S1, Supporting Information) were synthesized and confirmed by high-resolution mass spectometry (HRMS) and $^1$H and $^{13}$C NMR (Supporting Information). Their sensing properties were tested by chromatography plates containing these sensors and exposing the resulting sensors to C1−C4 alcohol vapors.

**Received:** November 3, 2013
**Accepted:** February 6, 2014
**Published:** February 6, 2014

   dx.doi.org/10.1021/ac403550t | *Anal. Chem.* 2014, 86, 2521−2525

## EXPERIMENTAL SECTION

**Materials and Methods.** All of the chemicals were purchased from commercial suppliers and used without further purification. All of the reactions were performed under an argon atmosphere using solvents purified by standard methods.

Melting points were measured on X-4 digital micro melting point analyzer. $^1$H and $^{13}$C NMR spectra were recorded on a Bruker 400 NMR spectrometer. Chemical shifts are reported in parts per million relative to tetramethylsilane (TMS) as the internal standard. Mass spectra were obtained on a high resolution mass spectrometer (IonSpec4.7 T FTMS-MALDI/DHB).

**Absorption Spectroscopy.** All spectral characterizations were carried out in HPLC-grade solvents at 20 °C within a 10 mm quartz cell. UV−vis absorption spectra were measured with a TU-1901 double-beam UV−vis spectrophotometer.

**Density Functional Theory Calculations.** Density functional theory (DFT) calculations using the Becke three-parameter exchange/Lee−Yang−Parr correlation hybrid functional (B3LYP) with 6-31G(d) basis sets as implemented in the Gaussian 09 suite of programs were carried out for the geometry optimizations of compounds **1**, **1′**, **2**, **2′**, **3**, and **3′**. The energies and oscillator strengths of the 80−120 lowest-energy electronic transitions were obtained by time-dependent (TD) DFT with the same basis sets.

**Synthesis of (E)-2-(2-Hydroxyphenylimino)1,8-naphthyridine (1).** 1,8-Naphthyridine-2-aldehyde (0.1059 g, 6.70 × $10^{-4}$ mol) and 2-aminophenol (0.0731 g, 6.70 × $10^{-4}$ mol) were mixed in 10 mL of ethanol, and the mixture was refluxed for 2 h under nitrogen atmosphere. After the solvent was removed under reduced pressure, the product was recrystallized from ethanol (0.1384 g, 83%). Characterization of **1**: mp = 199−201 °C. HRMS (EI) *m*/*z* calcd for $C_{15}H_{11}N_3ONa$ $[M + Na]^+$, 272.0794; found, 272.0799. $^1$H NMR (400 MHz, DMSO-$d_6$, TMS) $\delta_H$ 9.42 (s, 1H), 9.17 (d, 1H), 8.98 (s, 1H), 8.68 (m, 1H), 8.60 (m, 1H), 8.53 (m, 1H), 7.71 (m, 1H), 7.46 (m, 1H), 7.20 (m, 1H). 6.99 (m, 1H), and 6.92 (m, 1H). $^{13}$C NMR (100 MHz, DMSO-$d_6$) $\delta_C$ 159.24, 158.12, 155.85, 154.67, 152.47, 138.77, 137.98, 136.62, 129.57, 123.94, 123.61, 120.37, 120.14, and 117.04.

**Synthesis of (E)-2-(2-Hydroxyphenylimino)-4-methyl-7-acetamidyl-1,8-naphthyridine (2) and (E)-2-(2-Hydroxyphenylimino)-8-(oxygen acetate)-quinoline (3).** The synthetic procedure for **2** and **3** was similar to that for **1**, and the yields were 67% and 85%, respectively. Characterization of **2**: mp = 195−197 °C. HRMS (EI) *m*/*z* calcd for $C_{18}H_{16}N_4O_2$ $[M + H]^+$, 321.1352; found, 321.1346. $^1$H NMR (400 MHz, DMSO-$d_6$, TMS) $\delta_H$ 11.08 (s, 1H), 9.34 (s, 1H), 8.80 (s, 1H), 8.59 (m, 1H), 8.40 (m, 1H), 7.39 (m, 1H), 7.20 (m, 1H), 6.98 (m, 1H), 6.89 (m, 1H), 2.75 (s, 3H), and 2.20 (s, 3H). $^{13}$C NMR (100 MHz, DMSO-$d_6$) $\delta_C$ 170.69, 159.73, 157.51, 155.09, 154.81, 152.25, 146.93, 136.87, 136.59, 129.32, 121.13, 120.15, 120.10, 118.75, 116.95, 115.50, 24.68, and 18.39.

Characterization of **3**: mp = 159−160 °C. HRMS (EI) *m*/*z* calcd for $C_{20}H_{18}N_2O_4$ $[M + Na]^+$, 373.1159; found, 373.1169. $^1$H NMR (400 MHz, $CDCl_3$, TMS) $\delta_H$ 9.14(s, 1H), 8.38 (m, 1H), 8.25 (m, 1H), 7.50 (m, 1H), 7.42 (s, 1H), 7.26 (m, 2H), 7.04 (m, 2H), 6.96 (m, 2H), 5.02 (s, 2H), 4.31 (q, 2H), and 1.30 (t, 3H). $^{13}$C NMR (100 MHz, $CDCl_3$) $\delta_C$ 168.63, 157.50, 153.89, 153.61, 152.91, 139.96, 136.70, 134.36, 130.27, 127.93, 120.97, 120.40, 118.96, 116.40, 115.39, 110.25, 66.37, 61.57, and 14.22.

## RESULTS AND DISCUSSION

Figure 1 panels a−c show the absorption spectra of sensors **1**, **2** and **3** in 14 different solutions at a concentration of 1.5 × $10^{-5}$ M. The absorption bands in methanol, ethanol, *n*-propanol, and *n*-butanol solutions are located in the region 400−650 nm ($\lambda_{max}$ = 504, 522, 524, and 530 nm; molar extinction coefficient $\varepsilon$ = 1.3 × $10^4$, 0.6 × $10^4$, 1.3 × $10^4$, and 0.9 × $10^4$ $M^{-1}\cdot cm^{-1}$, respectively). Sensor **1** in other solvents including ethyl acetate, *N*,*N*-dimethylformamide (DMF), acetone, acetonitrile, tetrahydrofuran, chloroform, dichloromethane, pyridine, ether, and dimethyl sulfoxide (DMSO) is colorless, corresponding to absorption bands below 400 nm. As for **2** and **3**, similar results are obtained (Figure 1b,c). Figure 1panels d−f illustrate the colors of sensors **1**, **2**, and **3** in ethyl acetate, DMF, acetone, acetonitrile, methanol, ethanol, *n*-propanol, *n*-butanol, tetrahydrofuran, chloroform, dichloromethane, pyridine, ether, and DMSO under natural light, respectively. The dramatic difference in the absorption spectroscopy and color of sensors **1**, **2**, and **3** in different solvents may be ascribed to ground-state enol−keto tautomerism. Based on this signal transduction mechanism, these compounds can be applied as effective naked-eye-detectable alcohol sensors under solution or vapor conditions. As illustrated in Scheme 1, the proton transfer of the sensors between their enol and keto tautomers with C1−C4 alcohol's participation takes place through solvolysis. Hydrogen bonding between hydroxyl group of alcohols and N atom of Schiff base has played a crucial role in the proton transfer process. As for 2-propanol and isobutanol, similar absorption spectra of the three compounds were obtained (Figures S2−S4, Supporting Information). That is to say, sensors **1**, **2**, and **3** can also detect 2-propanol and isobutanol.

$^1$H NMR change demonstrated that isomer **1′** was formed (Figure 2) and the ratio of **1** to **1′** is 1/0.3. Upon addition of $CD_3OD$ into the DMSO-$d_6$ solution of **1**, six peaks at 9.11, 7.83, 6.75, 6.70, 6.55, and 6.0 appeared and the intensity increased with increasing $CD_3OD$ concentration. At the same

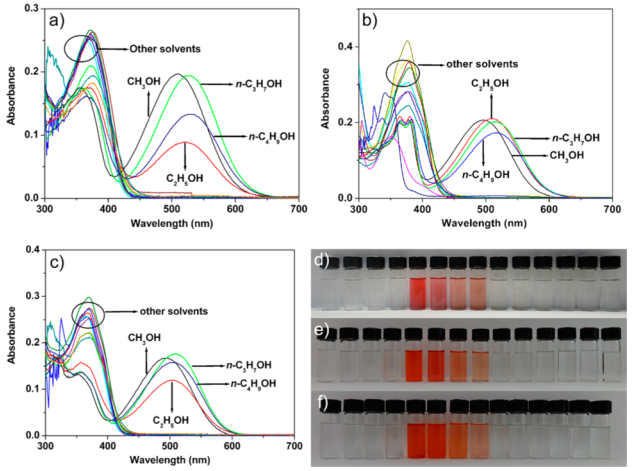


**Figure 1.** (a−c) Absorption spectroscopy of sensors **1**, **2**, and **3** (1.5 × $10^{-5}$ M) in different solvents (ethyl acetate, DMF, acetone, acetonitrile, methanol, ethanol, *n*-propanol, *n*-butanol, tetrahydrofuran, chloroform, dichloromethane, pyridine, ether, and DMSO). (d−f) Photographs of sensors **1**, **2**, and **3** (1.5 × $10^{-5}$ M) in different solvents (from left to right: ethyl acetate, DMF, acetone, acetonitrile, methanol, ethanol, *n*-propanol, *n*-butanol, tetrahydrofuran, chloroform, dichloromethane, pyridine, ether, and DMSO).


dx.doi.org/10.1021/ac403550t | Anal. Chem. 2014, 86, 2521−2525

**Scheme 1. Possible Proton Transfer Processes between Enol Sensors and Their Keto Tautomers in the Ground State**

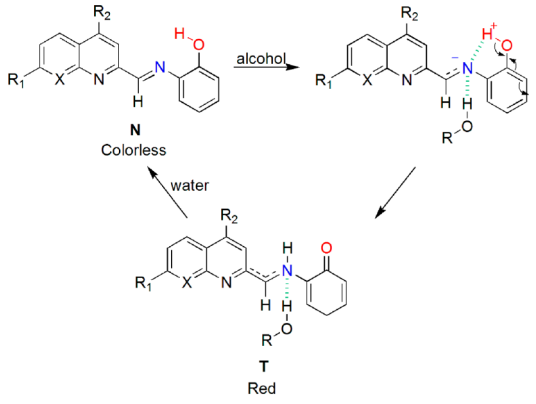


$R_1$ = H, $R_2$ = H, X = N **1**

$R_1$ = $NHCOCH_3$, $R_2$ = $CH_3$, X = N **2**

$R_1$ = H, $R_2$ = H, X = $HCOCH_2COOEt$ **3**

R = $C_nH_{2n}$, n = 1, 2, 3, and 4

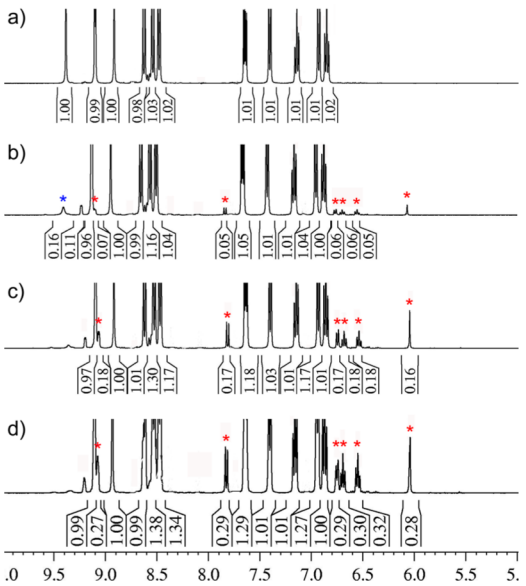


**Figure 2.** $^1$H NMR spectral change of sensor **1** in DMSO-$d_6$ upon addition of different amounts of $CD_3OD$ (a, 0 $\mu$L; b, 30 $\mu$L; c, 80 $\mu$L; d, 180 $\mu$L).

time, the intensity of the original peaks at 8.62, 8.53, 7.65, and 6.94 increased with the new peaks increasing. $^1$H NMR changes also show that ground-state tautomerism and intramolecular proton transfer existed and isomers **2′** and **3′** arose when $CD_3OD$ was added to DMSO-$d_6$ solutions of **2** and **3**, respectively (Figures S5 and S6, Supporting Information). The ratio of **2** to **2′** is 1/0.3, and that of **3** to **3′** is 1/0.2.

To further confirm the isomer structures and interpret the absorption properties, time-dependent density functional theory (TD-DFT) calculations were performed on this system. For each of **1**, **2**, and **3**, the highest occupied molecular orbital (HOMO) and the lowest unoccupied molecular orbital (LUMO) are similar, which is mainly located on benzene ring, naphthyridine (for **1** and **2**), and quinoline (for **3**) groups (Figure 3; Figures S7 and S8 in Supporting Information).

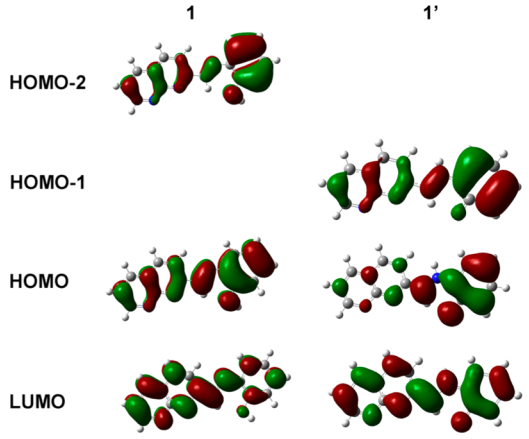


**Figure 3.** Frontier molecular orbitals of **1** and **1′** relevant to their transitions in 300−800 nm range.

However, for every isomer **1′**, **2′**, and **3′**, the HOMO is mainly located on the benzene ring, and the LUMO is similar to those of **1**, **2**, and **3**. The HOMO difference may be the reason for the absorption difference between each isomer pair.

As shown in Table 1 and Tables S1 and S2 in Supporting Information, the lowest energy transition of **1**, **2**, and **3** comes from HOMO to LUMO and the calculated excited wavelengths are 350.78, 356.84, and 359.49 nm, respectively. As for isomers **1′**, **2′**, and **3′**, the lowest energy transition comes from HOMO to LUMO, and the calculated excited wavelengths are 542.16, 543.16, and 533.99 nm. It is obvious that the lowest energy transitions for each pair of isomers are the same, while their calculated transition energies are very different. The calculated absorption-peak positions of isomers **1′**, **2′**, and **3′** are in good agreement with the experimental results (Figures S9−S11, Supporting Information), which further confirms the isomer structures.

**Table 1. Contributions of Various Orbital Transitions to the Lowest-Energy Transitions in 1 and 1′**

| | $\lambda_{ex}$, nm | | oscillator strength | |
|---|---|---|---|---|
| orbital transition | **1** | **1′** | **1** | **1′** |
| (HOMO − 2) → LUMO | | 362.11 | | 0.5471 |
| (HOMO − 1) → LUMO | 310.27 | | 0.1505 | |
| HOMO → LUMO | 350.78 | 542.16 | 0.5749 | 0.4768 |

Initially, the colorimetric sensing behavior of enol forms toward alcohol was investigated with a 1.5 × $10^{-5}$ M acetonitrile solution of alcohol sensors. Upon the addition of methanol, ethanol, *n*-propanol, and *n*-butanol, respectively, absorption peaks of sensor **1** at 504 nm (methanol), 522 nm (ethanol), 524 nm (*n*-propanol), and 530 nm (*n*-butanol) appeared and increased while the original absorption peak at 368 nm decreases (left panels of Figures S12−S15 in Supporting Information). Meanwhile, isosbestic points (414 nm for methanol, 407 nm for ethanol, 409 nm for *n*-propanol, and 409 nm for *n*-butanol) indicate the direct interconversion of both states of enol−keto isomers. Right panels of Figures S12−S15 (Supporting Information) show the relationship between concentration of alcohol in acetonitrile and absorption ratio. Similar absorption spectral changes of **2** and **3** were observed as for C1−C4 alcohols under analogous conditions (Figures S16−S23, Supporting Information). The absorption


dx.doi.org/10.1021/ac403550t | *Anal. Chem.* 2014, 86, 2521−2525

spectroscopy and isomers of sensors **1**, **2**, and **3** are reversible in different solvents, and trace amounts of C1−C4 alcohols with quite low concentrations have a dramatic effect on the absorption spectroscopy of acetonitrile solution of this series of sensors. For example, the addition of 0.3 vol % methanol to acetonitrile solution of the three sensors ($1.5 \times 10^{-5}$ M) respectively induced the absorbance peak intensities at 504 nm (**1** and **2**) and 489 nm (**3**) to increase more than 10-fold. As for 2-propanol and isobutanol, addition of 2-propanol/isobutanol can also make a new absorption peak appear, demonstrating an interconversion of both states of enol-keto isomers (Figures S24−S26, Supporting Information).

Upon slow addition of water to the respective alcohol solutions, the absorbance peak intensities of sensors **1**, **2**, and **3** in the range 400−650 nm decreased, except the absorption spectral change of **3** ($1.5 \times 10^{-5}$ M) in methanol upon addition of water and absorbance intensity is linearly proportional to the volume ratio of water to alcohol (see Figure 4 and Figure S27−S35 in Supporting Information). Absorption spectral changes are the result of a keto−enol transformation. Slow volatilization of the above solution containing **3** gave the enol tautomer crystal structure (Figure 5), which further confirmed the reversibility of the keto−enol transformation process. The colors of sensors **1**, **2**, and **3** in ethanol display a very quick response to water. The color is red when concentration is equal or larger than 99.5% and fades dramatically accompanied with the concentration decrease (Figure 6). The solvents are almost colorless when the concentration is smaller than 95%, implying that they can be applied as alcohol concentration indicators in water-removal distillation. As for 2-propanol and isobutanol, addition of water into the 2-propanol/isobutanol solutions of the three sensors respectively can also result in an interconversion from keto to enol isomer (Figures S36−S38, Supporting Information).

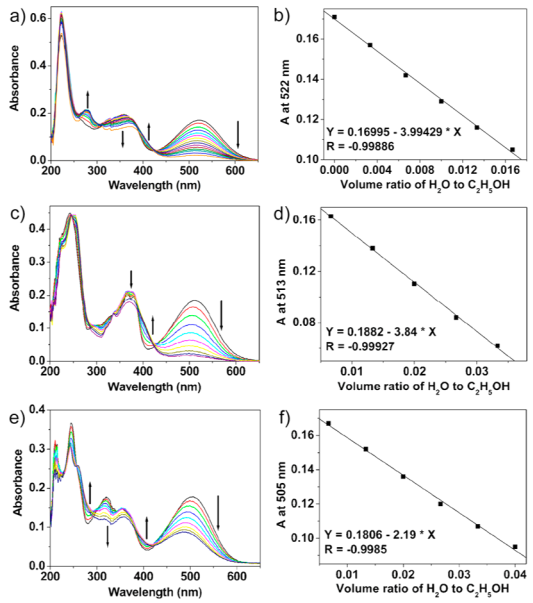


**Figure 4.** (a, c, e) Absorption spectral changes of sensors **1**, **2**, and **3** ($1.5 \times 10^{-5}$ M) in ethanol upon addition of water, respectively. (b, d, f) Plot of absorbance intensity of **1**, **2**, and **3** ($1.5 \times 10^{-5}$ M, ethanol) as a function of ethanol concentration, respectively. *A* represents absorbance.

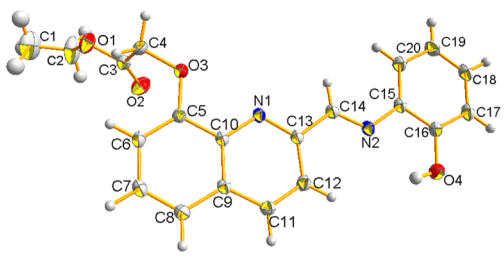


**Figure 5.** X-ray crystal structure of **3** (CCDC structure 960149).

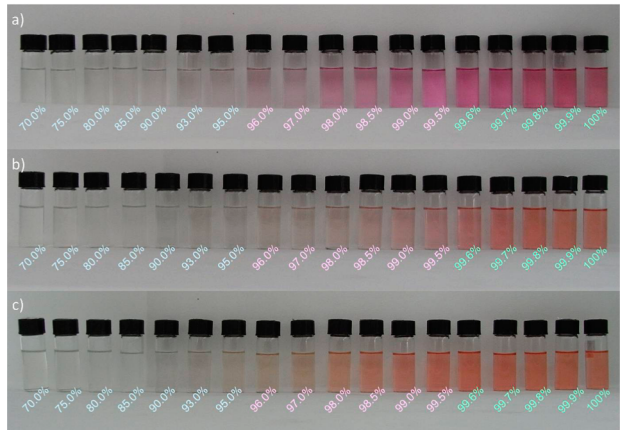


**Figure 6.** (a−c) Photographs of sensors **1**, **2** and **3** ($1.5 \times 10^{-5}$ M) in different concentration alcohol solutions, respectively.

The detection of C1−C4 alcohol vapors on chromatography plates containing 0.1% (w/w) **1**, **2**, and **3** sensors was carried out successfully. Upon exposure to different alcohol vapors, the concentration-dependent dramatic color changes from pale yellow to red were observed, which could be ascribed to the ground-state intramolecular proton transfer and tautomerism (Figure S39, Supporting Information). When the profile of chromatography plates containing colorimetric sensors was exposed to a flux of pure $N_2$ alternated with a flux of C1−C4 alcohol in $N_2$, the color changes were fast and reversible.

## CONCLUSION

This work demonstrates that it is possible to prepare alcohol sensors based on ground-state intramolecular proton transfer and tautomerism strategies. Hydrogen bonding between alcohol and colorimetric sensor induces significant color changes from colorless to red. Reverse proton transfer in the ground state induced by water achieves a fully reversible reaction. Solvent color indicating alcohol concentration is more suitable for direct observation with the naked eye. This novel approach via chemical structural changes can be useful for rational design of many different colorimetric sensors toward organic analytes, and these sensors could be used as indicators in water removal experiments.

## ASSOCIATED CONTENT

### Supporting Information

Thirty-nine figures and two tables giving additional experimental details as described in the text, including spectral data, images of chromatography plates, and contributions of various orbital transitions (PDF); crystallographic data (CIF). This


dx.doi.org/10.1021/ac403550t | *Anal. Chem.* 2014, 86, 2521−2525

material is available free of charge via the Internet at http://pubs.acs.org.

## AUTHOR INFORMATION


### Corresponding Authors

*Fax 86 371-67781205; e-mail lizx@zzu.edu.cn.
*Fax 86 371-67781205; e-mail yumm@zzu.edu.cn


### Notes

The authors declare no competing financial interest.

## ACKNOWLEDGMENTS

This work was supported by NSFC (50903075) and Specialized Research Fund for the Doctoral Program of Higher Education (20114101120003).

## REFERENCES


(1) (a) Thorson, M. K.; Majtan, T.; Kraus, J. P.; Barrios, A. M. *Angew. Chem., Int. Ed.* **2013**, *52*, 4641−4644. (b) Yuan, L.; Lin, W. Y.; Xie, Y. N.; Chen, B.; Zhu, S. S. *J. Am. Chem. Soc.* **2012**, *134*, 1305−1315. (c) Santos-Figueroa, L. E.; Moragues, M. E.; Climent, E.; Agostini, A.; Martinez-Manez, R.; Sancenon, F. *Chem. Soc. Rev.* **2013**, *42*, 3489−3613. (d) Lee, M. H.; Yang, Z.; Lim, C. W.; Lee, Y. H.; Dongbang, S.; Kang, C.; Kim, J. S. *Chem. Rev.* **2013**, *113*, 5071−5109.

(2) Pinalli, R.; Nachtigall, F. F.; Ugozzoli, F.; Dalcanale, E. *Angew. Chem., Int. Ed.* **1999**, *38*, 2377−2380.

(3) Suman, M.; Freddi, M.; Massera, C.; Ugozzoli, F.; Dalcanale, E. *J. Am. Chem. Soc.* **2003**, *125*, 12068−12069.

(4) Melegari, M.; Suman, M.; Pirondini, L.; Moiani, D.; Massera, C.; Ugozzoli, F.; Kalenius, E.; Vainiotalo, P.; Mulatier, J. C.; Dutasta, J. P.; Dalcanale, E. *Chem.—Eur. J.* **2008**, *14*, 5772−5779.

(5) (a) Pirondini, L.; Dalcanale, E. *Chem. Soc. Rev.* **2007**, *36*, 687−699. (b) Pinalli, R.; Dalcanale, E. *Acc. Chem. Res.* **2013**, *46*, 399−411.

(6) Maffei, F.; Betti, P.; Genovese, D.; Montalti, M.; Prodi, L.; De Zorzi, R.; Geremia, S.; Dalcanale, E. *Angew. Chem., Int. Ed.* **2011**, *50*, 4654−4657.

(7) (a) Liu, X. H.; Li, J. S.; Hu, C.; Zhou, Q.; Zhang, W.; Hu, M. R.; Zhou, J. Z.; Wang, J. Y. *Angew. Chem., Int. Ed.* **2013**, *52*, 4805−4809. (b) Palacios, M. A.; Wang, Z.; Montes, V. A.; Zyryanov, G. V.; Anzenbacher, P. *J. Am. Chem. Soc.* **2008**, *130*, 10307−10314. (c) Xu, Z.; Baek, K. H.; Kim, H. N.; Cui, J.; Qian, X.; Spring, D. R.; Shin, I.; Yoon, J. *J. Am. Chem. Soc.* **2010**, *132*, 601−610.

(8) (a) Hong, C. F.; Hagihara, M.; Nakatani, K. *Angew. Chem., Int. Ed.* **2012**, *51*, 9389−9392. (b) Dohno, C.; Kohyama, I.; Hong, C. F.; Nakatani, K. *Nucleic Acids Res.* **2012**, *40*, 2771−2781. (c) Takei, F.; Igarashi, M.; Hagihara, M.; Oka, Y.; Soya, Y.; Nakatani, K. *Angew. Chem., Int. Ed.* **2009**, *48*, 7822−7824.

(9) (a) de Greef, T. F. A.; Ercolani, G.; Ligthart, G. B. W. L.; Meijer, E. W.; Sijbesma, R. P. *J. Am. Chem. Soc.* **2008**, *130*, 13755−13764. (b) Minakawa, N.; Ogata, S.; Takahashi, M.; Matsuda, A. *J. Am. Chem. Soc.* **2009**, *131*, 1644−1645. (c) Li, Y.; Park, T.; Quansah, J. K.; Zimmerman, S. C. *J. Am. Chem. Soc.* **2011**, *133*, 17118−17121.

(10) Ismayilov, R. H.; Wang, W. Z.; Lee, G. H.; Yeh, C. Y.; Hua, S. A.; Song, Y.; Rohmer, M. M.; Benard, M.; Peng, S. M. *Angew. Chem., Int. Ed.* **2011**, *50*, 2045−2048.

(11) (a) Das, R. K.; Saha, B.; Rahaman, S. M. W.; Bera, J. K. *Chem.—Eur. J.* **2010**, *16*, 14459−14468. (b) Saha, B.; Ghatak, T.; Sinha, A.; Rahaman, S. M. W.; Bera, J. K. *Organometallics* **2011**, *30*, 2051−2058.

(12) (a) Yu, M. M.; Li, Z. X.; Wei, L. H.; Wei, D. H.; Tang, M. S. *Org. Lett.* **2008**, *10*, 5115−5118. (b) Li, Z. X.; Yu, M. M.; Zhang, L. F.; Yu, M.; Liu, J. X.; Wei, L. H.; Zhang, H. Y. *Chem. Commun.* **2010**, *46*, 7169−7171. (c) Li, Z. X.; Zhao, W. Y.; Li, X. Y.; Zhu, Y. Y.; Liu, C. M.; Wang, L. N.; Yu, M. M.; Wei, L. H.; Tang, M. S.; Zhang, H. Y. *Inorg. Chem.* **2012**, *51*, 12444−12449.

(13) (a) Weinberg, D. R.; Gagliardi, C. J.; Hull, J. F.; Murphy, C. F.; Kent, C. A.; Westlake, B. C.; Paul, A.; Ess, D. H.; McCafferty, D. G.; Meyer, T. J. *Chem. Rev.* **2012**, *112*, 4016−4093. (b) Warren, M. M.; Kaucikas, M.; Fitzpatrick, A.; Champion, P.; Sage, J. T.; van Thor, J. J. *Nat. Commun.* **2013**, *4*, 1461. (c) Eustis, S. N.; Radisic, D.; Bowen, K. H.; Bachorz, R. A.; Haranczyk, M.; Schenter, G. K.; Gutowski, M. *Science* **2008**, *319*, 936−939.

(14) (a) Baranov, M. S.; Lukyanov, K. A.; Borissova, A. O.; Shamir, J.; Kosenkov, D.; Slipchenko, L. V.; Tolbert, L. M.; Yampolsky, I. V.; Solntsev, K. M. *J. Am. Chem. Soc.* **2012**, *134*, 6025−6032. (b) Tolbert, L. M.; Solntsev, K. M. *Acc. Chem. Res.* **2002**, *35*, 19−27. (c) Waluk, J. *Acc. Chem. Res.* **2003**, *36*, 832−838.

(15) (a) Wang, J. F.; Chu, Q. H.; Liu, X. M.; Wesdemiotis, C.; Pang, Y. *J. Phys. Chem. B* **2013**, *117*, 4127−4133. (b) Yang, Y. M.; Zhao, Q.; Feng, W.; Li, F. Y. *Chem. Rev.* **2013**, *113*, 192−270.

(16) Chipem, F. A. S.; Krishnamoorthy, G. *J. Phys. Chem. A* **2009**, *113*, 12063−12070.

(17) (a) Brenlla, A.; Veiga, M.; Lustres, J. L. P.; Rodriguez, M. C. R.; Rodriguez-Prieto, F.; Mosquera, M. *J. Phys. Chem. B* **2013**, *117*, 884−896. (b) Park, S. Y.; Kim, Y.; Lee, J. Y.; Jang, D. J. *J. Phys. Chem. B* **2012**, *116*, 10915−10921.

(18) Brenlla, A.; Rodriguez-Prieto, F.; Mosquera, M.; Rios, M. A.; Rodriguez, M. C. R. *J. Phys. Chem. A* **2009**, *113*, 56−67.

(19) (a) Liu, X. J.; Ngo, H. T.; Ge, Z. J.; Butler, S. J.; Jolliffe, K. A. *Chem. Sci.* **2013**, *4*, 1680−1686. (b) Maue, M.; Schrader, T. *Angew. Chem., Int. Ed.* **2005**, *44*, 2265−2270.